Determining Fermi Weak Coupling Constant Using Muon Decay Analysis

Isaiah Mumaw*
University of Notre Dame
Jordan Hall Advanced Physics Lab

Jamie Harkin, Caroline Melancon, Colin Pifer
(Dated: November 26, 2021)

When muons decay, they produce two neutrinos and an electron. The high-energy incident muon and its lower-energy resultant electron can both be detected inside of a scintillator, with the signals from each being divided and temporally offset. The resultant time differentials from thousands of these muon decays can be plotted, allowing us to calculate the mean decay time τ of muons by fitting a decaying exponential. From this mean decay time, we are able to calculate the Fermi weak coupling constant G_F. We calculated $\tau_{\text{exp}} = 2.157 \pm 0.015$ µs and $G_{F,\text{exp}}/(\hbar c)^3 = (1.175 \pm 0.004) \times 10^{-5}/\text{GeV}^2$.

I. BACKGROUND

A. Muon Production and Decay

Interactions between cosmic rays and particles in the upper atmosphere produce a variety of particles, such as pions, kaons, and high-energy nuclei. The majority of these attenuate in the atmosphere before reaching Earth's surface [1], however, some of these particles will decay into muons, with a mean lifetime of [2]:

$$\tau_{\mu,\text{theoretical}} = 2.1969811 \pm 0.0000022 \text{ µs}. \quad (1)$$

Without relativistic effects, this lifetime is still far too short to reach Earth's surface. However, because a typical muon will have speeds in the hyper-relativistic realm, its range often extends far below the surface of the Earth. On average, muons are able to reach Earth's surface at a rate of 0.01 muons per second per square centimeter per steradian [1].

As a muon decays, it produces a ν_μ and W^- boson, the latter of these subsequently decaying into an e^- and $\overline{\nu}_e$ [3]. This process is shown in Fig. 1.

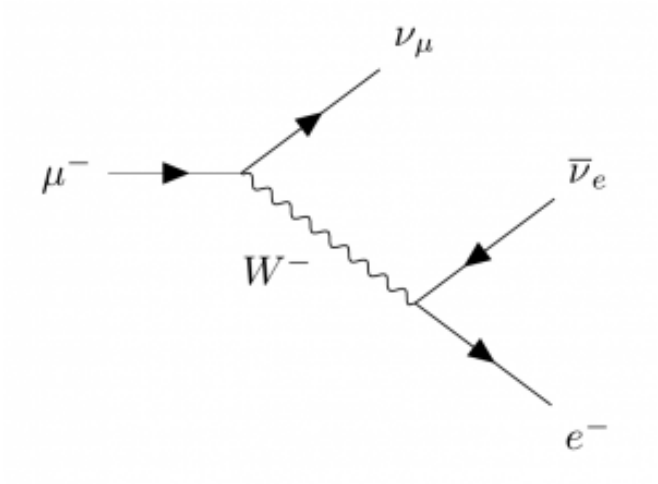

FIG. 1. Feynman diagram for muon decay process. Muons typically decay after approximately 2.1969811 ± 0.0000022 µs [2, 3].

B. The Weak Force

The four fundamental forces are the most basic known interactions in the universe. One of these interactions, the weak force, governs the exchange of the intermediate vector bosons, W and Z. These particles are key to numerous processes including the decay of muons [4].

The coupling constant for muon decays is given as the Fermi weak coupling constant, G_F, defined as:

$$\frac{G_F}{(\hbar c)^3} = \frac{\sqrt{2}}{8}\left(\frac{g_w}{M_W c^2}\right)^2 = 1.116 \times 10^{-5}/\text{GeV}^2, \quad (2)$$

where M_W is the mass of a W boson and g_w is the weak coupling constant, given as $\sqrt{4\pi\alpha_w}$, where α_w is a scaling factor specific to W bosons [5].

Using this, we can derive the equation for the theoretical muon lifetime:

$$\tau = \left(\frac{(\hbar c)^3}{G_F}\right)^2 \frac{192\pi^3\hbar}{(m_\mu c^2)^5}, \quad (3)$$

where m_μ is the muon mass, c is the speed of light, and $\hbar$ is the reduced Planck constant [5].

While G_F cannot be measured directly, it is possible to measure muon decays and use the detected lifetime to acquire G_F experimentally.

II. EXPERIMENTAL SETUP

Incident muons and the resultant electrons produced during their decay were detected using a fast plastic scin-

* imumaw@nd.edu

tillator (Detector). This detector was powered by a high voltage source (HV). Outgoing signals from the detector were amplified using a photomultiplier (PM) and split using a voltage divider (DIV), creating two separate but identical output signals.

One signal was sent to an oscilloscope. This was done to visualize the energy difference between the high energy incident muon and low energy resultant electron. These appeared as two separate peaks on the oscilloscope screen.

The second outgoing signal was split again between two constant fraction discriminators (CFD-A and CFD-B). The lower level discriminator (LLD) on CFD-A was set to a high value in order to focus only on incoming muons, specifically those with hyper-relativistic velocities, and the LLD on CFD-B was set to a low value in order to allow signals from the resultant electrons to get through. These values were chosen based on the peaks heights on the oscilloscope. The signal from CFD-A was also delayed by approximately 60 ns in order to prevent overlap with signals from CFD-B. This was done using a roughly 60 foot length of wire, assuming signal propagation nearly equal to light speed.

The signal from CFD-A was then fed into the start input of the time to amplitude converter (TAC), with signal from CFD-B being fed into the stop input. Assuming that the input from CFD-A aligned with an input from CFD-B, then the time difference between these two signals was then converted to a voltage. Using a multichannel analyzer (MCA) this voltage was converted into a digital signal broken up into discrete channels, allowing the computer (Comp) to read and display them.

The block diagram for this entire process is shown in Fig. 2.

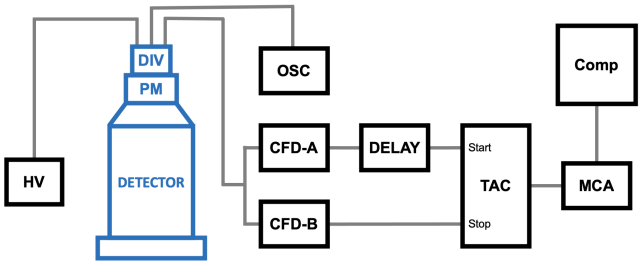

FIG. 2. Block diagram of experimental setup. Data collected from the scintillator was sent to both an oscilloscope a pair of constant fraction discriminator's, the first being offset by 60 ns to prevent overlap. The time difference was then converted to channels and sent to the computer to display.

III. RESULTS AND ANALYSIS

Data for each trial was collected over the course of two weeks, as the number of detected muons that fell under our constraints averaged out to less than 10 per minute. The results took the form of a decaying exponential.

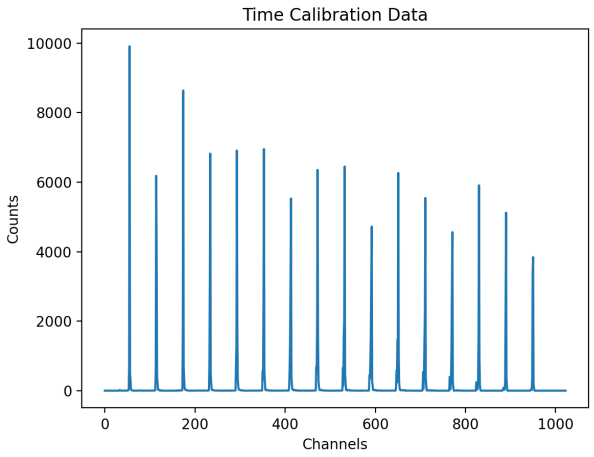

FIG. 3. Results using time calibration module. Peaks were separated by a period of 0.64 µs. These results can be used to find the ratio between channels and µs.

Resultant data was scaled from channels to µs using a time calibration module. This module gave a series of peaks separated by a period of 0.64 µs, as shown in Fig. 3.

The precise peak was calculated by taking a weighted average of channels around each peak. By plotting these peaks with respect to the period, we were able to find a relationship between the data using linear regression. The slope of the fit line, then, gave the ratio between channels and time. This plot is shown in Fig. 4.

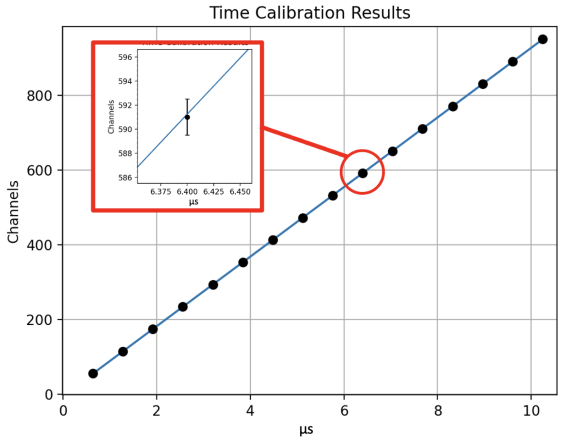

FIG. 4. Plot of peak channel vs. number of µs. The line of fit was found using linear regression, with the slope giving the ratio between channels and µs. This ratio was found to be: 93.147 ± 0.022 channels per µs.

The ratio between channels and µs was calculated to be:

$$\eta = 93.147 \pm 0.022 \ \frac{\text{channels}}{\mu\text{s}}. \tag{4}$$

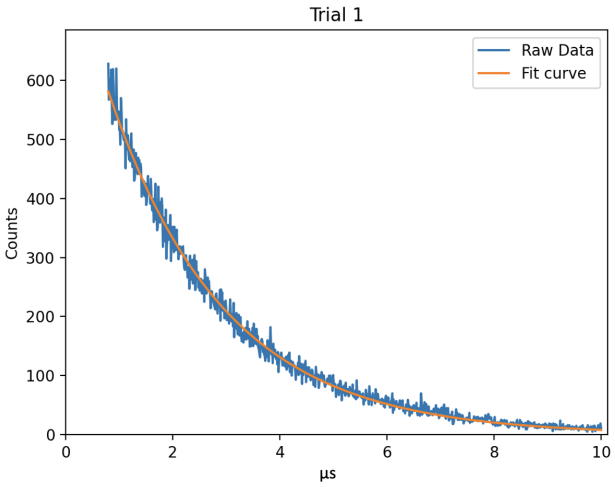

FIG. 5. Resultant data from the first trial. The fit line was calculated based on a decaying exponential, and the x-axis has been scaled to μs.

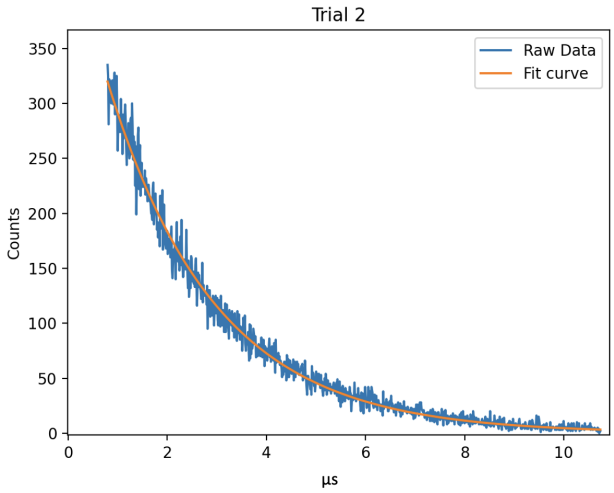

FIG. 6. Resultant data from the second trial. This trial had a higher cutoff for incoming muons, thus focusing on more relativistic interactions.

After using η to scale the data to μs, the results were fit to a decaying exponential of the form:

$$f(t) = Ae^{-t/\tau} + B, \tag{5}$$

where τ is the mean muon lifetime and A is a constant that scales for both the total number of counts as well as the length of the scintillator. We assumed that $B = 0$ because as t approaches infinity, the number of muons decaying in such a time frame should approach 0 (and the fitted data reflected this, with very small calculated values for B).

The resultant data and fit curves from each trial are shown in Fig. 5 and Fig. 6. Fit curves were determined using non-linear least squares, and the resulting fit parameters are listed in Table I.

TABLE I. Calculated fit parameters for both trials. Parameters were calculated using non-linear least squares.

Trial	τ (μs)	A
1	2.152 ± 0.009	841.047 ± 3.577
2	2.161 ± 0.012	462.032 ± 2.524

We then averaged the resultant values for τ, giving us an overall experimental decay time of:

$$\tau_{\text{exp}} = 2.157 \pm 0.015 \text{ μs}. \tag{6}$$

By rearranging Eq. 3, we then calculated the value of $G_{F,\text{exp}}$:

$$\frac{G_{F,\text{exp}}}{(\hbar c)^3} = \sqrt{\frac{1}{\tau}\frac{192\pi^3\hbar}{(m_\mu c^2)^5}} \tag{7}$$

$$\frac{G_{F,\text{exp}}}{(\hbar c)^3} = (1.175 \pm 0.004) \times 10^{-5}/\text{GeV}^2. \tag{8}$$

Error values for both τ_{exp} and $G_{F,\text{exp}}/(\hbar c)^3$ were calculated using standard error propagation methods.

IV. DISCUSSION

These results were within 3σ of the theoretical calculation of τ, differing from the expectation by less than 2%, and within 14σ of the theoretical calculation of $G_F/(\hbar c)^3$, differing from the expectation by roughly 5%.

The primary source of error here was due to calibration of the CFD's and random variations in incident muon energy. Muons that reach Earth's surface are almost always relativistic, however the energies can still vary greatly, resulting in incoming signals taking on a wide range. While the CFD's are partially able to account for this, in reality the LLD is set simply based on visual inspection of the oscilloscope. While these effects can be countered by increasing the LLD on CFD-A, the drawback is that data takes substantially longer to be collected. Therefore, the incoming muons will give results that slightly underestimate τ, simply because there are less relativistic and therefore much more likely to decay within the scintillator.

There are several methods that may be able to mitigate this problem within the limits of the setup. One could run a trial for much longer with a high LLD on CFD-A, or alternatively find a relation between the LLD and τ over several trials and approximate the true value of τ. Either way, these corrections should result in more accurate calculations of $G_F/(\hbar c)^3$.

Muon research is an actively growing field at the forefront of physics. While the Standard Model is well established as our best formulation of particle physics, it fails in a number of key aspects. Various research teams are working on expanding and adjusting the model, with some of these teams experimenting on muons as a way of uncovering new information. More broadly, the weak force allows for understanding of numerous natural processes ranging from beta decay to nuclear fusion, and is being used in modern research to understand other particles, such as the Higgs Boson.

V. ACKNOWLEDGEMENTS

We extend our gratitude to the University of Notre Dame and its physics department for the use of their facilities while working on this experiment. We also thank Professor William Zech and our TAs Sam Porter and Will von Seeger, for providing us with guidance and assistance throughout the process.

[1] *Muon Basics.* Universidad Nacional de La Plata. Retrieved November 2, 2021, from http://www2.fisica.unlp.edu.ar

[2] J. Beringer et al. (2012). *Leptons.* Particle Data Group. Retrieved November 2, 2021, from https://pdg.lbl.gov/2012/tables/rpp2012-sum-leptons.pdf

[3] Dobbs, A. (2017, September 1). *General Infromation - MICE.* Imperial College London. Retrieved November 2, 2021, from https://blogs.imperial.ac.uk/mice/category/general-information/

[4] Nave, R. *Fundamental Forces.* Hyperphysics. Retrieved November 4, 2021, from http://hyperphysics.phy-astr.gsu.edu/hbase/Forces/funfor.html

[5] Griffiths, D. (2008). *Introduction to Elementary Particles: Second Edition.* Wiley-VCH. PDF version: https://mikefragugliacom.files.wordpress.com/2016/12/introduction-to-elementary-particles-gnv64.pdf